ELSEVIER

The Chemical Engineering Journal 57 (1995) 115–125

THE CHEMICAL ENGINEERING JOURNAL

The use of the dusty-gas model for the description of mass transport with chemical reaction in porous media

J.W. Veldsink [a,1], R.M.J. van Damme [b], G.F. Versteeg [a], W.P.M. van Swaaij [a]

[a] *Department of Chemical Engineering, University of Twente, P.O. Box 217, 7500 AE Enschede, Netherlands*

[b] *Department of Applied Mathematics, University of Twente, P.O. Box 217, 7500 AE Enschede, Netherlands*

Abstract

In the present study, mass transport accompanied by chemical reactions in porous media is studied according to the Fick model and the dusty-gas model. For mass transport accompanied by a chemical reaction in catalyst structures showing a plane, line, or point of symmetry, the approximate analytical concept of an effectiveness factor, accounting for intraparticle diffusion, was also evaluated. For a variety of reaction schemes and kinetic rate equations, a comparison was made between the results of the numerical models (Fick and dusty-gas) and the effectiveness-factor concept.

From the results it was concluded that pressure in porous catalyst with a plane, line, or point of symmetry did not affect the fluxes seriously, and, therefore, the pressure-driven flow can be omitted from the flux expression without significant loss of accuracy. Furthermore, both for single and multiple reactions, the Fick model is satisfactorily accurate to estimate the transport rate in all cases, and the results deviate only slightly from the dusty-gas model. It should be noted that this latter model requires substantially more computational time.

For catalytic membranes, however, transport of inert components as well as large trans-membrane pressure differences may be present, which affect the transport of the reactants and products. The calculations showed that, in contrast to the above-mentioned structures, in this case the dusty-gas model has to be used to describe the transport.

Keywords: Dusty-gas model; Mass transport; Porous media; Fick model

1. Introduction

Simultaneous transport and reaction in porous catalyst has been widely studied over the years and is described in many textbooks [1,2]. The transport of components into the porous matrix can be described according to the Fick model or the dusty-gas model. Since the Fick model is simpler than the dusty-gas model, it is, therefore, more frequently used. Close inspection of the model equations reveals that the Fick model is basically an asymptotic case of the dusty-gas model.

Numerous studies on transport through porous media in the absence of a chemical reaction reveal that the dusty-gas model is superior to the Fick model in its ability to predict the fluxes (see Refs. [3,4]). Especially in porous catalysts, the Fick model, however, is still frequently used, because its simplicity allows explicit, analytical expressions to be derived for the fluxes. These can be obtained from the dusty-gas model only for a binary mixture or after a strong reduction of the original equations [5].

If pressure gradients occur in a porous matrix, additional, convective transport should be taken into account, which is a natural extension of the dusty-gas model. Non-uniform pressure profiles in porous catalyst can be induced by reactions involving a change in the number of molecules. Kehoe and Aris [6] and Hite and Jackson [7] showed that the dusty-gas model could be successfully applied to predict the fluxes for these reactions. Davies et al. [8] demonstrated that the prediction of the effectiveness factor was in good agreement with experimental values for the SO_2 oxidation reaction. Owing to the presence of large pressure gradients and a net molar outflux of reactants, Bliek et al. [9] used the dusty-gas model in the coal gasification reaction, and, for similar reasons, Gonzalez et al. [10] used this model for the methane-reforming reaction. Graaf et

[1] Present address: Dept. of Chemical Engineering, University of Groningen, Nijenborgh 4, 9747 AG, Groningen, The Netherlands.

[2] Details of the numerical procedure are available on request from the first author.

al. [11] evaluated kinetic data of the methanol process on the basis of the dusty-gas model. Recently, Sloot et al. [12] developed a macroporous, catalytic membrane reactor and demonstrated that convective motion attributed several attractive features to this type of reactor. As a consequence of the convective transport, the fluxes through their membrane reactor should be calculated according to the dusty-gas model.

The present study compares the results of the Fick model with the dusty-gas model for the description of transport and reaction in porous catalyst. First, catalyst geometries with a plane, line, or point of symmetry are studied, and secondly a slab geometry with different interface compositions, thus resembling a membrane reactor. The present studies include irreversible, reversible, single and multiple reactions. Therefore it can be seen as an extension to other studies, such as Refs. [6,7,12]. Since the transport in porous media generally occurs in the transition region between Knudsen and continuum diffusion, the calculations were restricted to this regime.

2. Basic model equations for mass transport with chemical reaction

In a porous medium the transport of components, accompanied by chemical reactions, is determined by the local conservation of mass for each participating component. For a single component i the result is

$$\frac{\epsilon}{RT}\frac{\partial(x_iP)}{\partial t} = -\nabla\cdot N_i + R_i \qquad (\text{mol m}_{\text{cat}}^{-3}\ \text{s}^{-1}) \tag{1}$$

In Eq. (1), R_i represents the local consumption or production rate according to an arbitrary kinetic rate equation. This kinetic rate expression is usually determined experimentally and is an explicitly known function of the partial pressures of the components and temperature:

$$R_i = f(T, p_1 ...) \text{ and } R_{\text{inert}} = 0 \qquad (\text{mol m}_{\text{cat}}^{-3}\ \text{s}^{-1}) \tag{2}$$

For reasons of simplicity, the equations are represented for a slab geometry (Cartesian coordinates) hereafter. Whenever different catalyst geometries (sphere, cylinder, slab) are discussed, the appropriate form of the differential operator was used in Eq. (1). In all cases the transport was considered as one-dimensional.

Transport of the components, N_i, is due to mole-fraction gradients, a total pressure gradient, and there may be additional transport along the surface as well. However, since surface diffusion is observed only for a few special systems or conditions [4,13], it is neglected in the present study. Furthermore the transport is assumed to proceed isothermally.

2.1. Flux models

The simplest model to describe transport of components through the gas phase is the Fick model (FM), which describes the transport as a product of a diffusion coefficient and the partial-pressure gradient of the particular component,

$$N_i = \frac{-D_i^e}{RT}\frac{\partial(x_iP)}{\partial z} \qquad (i = 1...n)\ (\text{FM}) \tag{3}$$

The diffusion process is bound to two asymptotic regimes. In small pores the molecule–wall interactions determine the process (Knudsen diffusion) and, in free space, molecule–molecule interactions are important (continuum/bulk/molecular diffusion). In each of these regimes a distinct diffusion coefficient prevails, and to evaluate the diffusion coefficient in the transition region, the Bosanquet formula can be used:

$$D_i^e = \left(\frac{1}{D_{i,\text{m}}^e} + \frac{1}{D_{i,\text{k}}^e}\right)^{-1} \tag{4a}$$

If the mixture continuum diffusivity is unknown, it can be estimated using the diffusivity of component i in all other components present in the mixture (Blanc's law):

$$D_{i,\text{m}}^e = \frac{1}{(1-x_i)}\sum_{j=1,\, j\neq i}^{n} D_{ij}^e x_j \tag{4b}$$

The diffusion coefficients are effective diffusivities prevailing in the particular medium and calculated according to

$$D_{i,\text{k}}^e = \frac{4}{3}K_0\left(\frac{8RT}{\pi M_i}\right)^{1/2} \qquad (\text{m}^2\ \text{s}^{-1}) \tag{5a}$$

$$D_{ij}^e = \frac{\epsilon}{\tau}D_{ij}^0 \qquad (\text{m}^2\ \text{s}^{-1}) \tag{5b}$$

When a pressure gradient contributes to the total transport, it is possible to add the d'Arcy equation to the diffusional transport, resulting in an extended Fick model:

$$N_i = \frac{1}{RT}\left(D_i^e\frac{\partial(x_iP)}{\partial z} + \frac{B_0x_iP}{\mu}\frac{\partial P}{\partial z}\right) \qquad (i-1...n)(\text{extended FM}) \tag{6}$$

In the dusty-gas model (DGM) the diffusive transport is described by the Stefan–Maxwell diffusion equations, and the convective motion is implemented in the flux equations directly from the beginning. Concise monographs which describe the historical background and the derivation of the model equations are presented by Refs. [5,14]. The flux expression for a single species i according to the DGM results in

$$\sum_{j=1,\, j\neq i}^{n} \frac{x_i N_j - x_j N_i}{P D_{ij}^{e}} - \frac{N_i}{P D_{i,k}^{e}} \tag{7}$$

$$= \frac{1}{RT}\frac{\partial x_i}{\partial z} + \frac{x_i}{PRT}\left(\frac{B_0 P}{\mu D_{i,k}^{e}} + 1\right)\frac{\partial P}{\partial z}$$

$$(i = 1...n) \text{ (DGM)}$$

with diffusion coefficients according to Eqs. (5a) and (5b).

Generally, it is not possible to derive an explicit equation for N_i, such as Eq. (3). Hence, the incorporation of the DGM complicates the solution of Eq. (1) severely. Therefore, early work on the DGM was restricted to binary systems, or approximations had to be made in order to solve the mass balances [5]. For binary systems and in the absence of a pressure gradient, the DGM can be rewritten as

$$N_A = \frac{1}{RT}\left(\frac{(1-\gamma x_A)}{D_{AB}^{e}} + \frac{1}{D_{A,K}^{e}}\right)^{-1}\frac{\partial P_A}{\mathrm{d}z}$$

$$\text{with } \gamma = 1 + N_B/N_A \tag{8}$$

where $\gamma = 1 + N_B/N_A$. However, powerful computers are available and generally accessible nowadays, so the numerical solution of the complete set of partial differential equations (1) with the fluxes expressed according to the DGM is feasible.

The structure of the porous medium is characterized by three effective parameters, K_0, B_0 and ϵ/τ (see Eqs. (4)–(7)), which usually have to be determined experimentally. This minimum number of structure parameters is based on the assumption that the structure of the porous medium is homogeneous. Several more sophisticated models dealing with all kinds of heteroporosity have been proposed, but unless more specific information about the pore geometry is available, the assumption of homoporosity is usually sufficiently accurate [4,15,16].

The model described by the set of equations (1) and (2) together with either Eq. (3), Eq. (6) or Eq. (7) consists of n independent mass conservation equations, but contains $n+1$ variables (n mole fractions and the total pressure). Therefore, the summation of mole fractions was used to complete the model

$$\sum_{i=1}^{n} x_i = 1 \tag{9}$$

To solve Eq. (1) uniquely, proper initial and boundary conditions are required, which are usually of the fixed (Dirichlet) type:

$$t = 0: P_i(0,z) = P_i(z) \quad \forall z, i = 1...n \tag{10a}$$

$$z = 0: P_i(t,0) = P_i(0) \quad \forall t, i = 1...n \tag{10b}$$

$$z = L: P_i(t,L) = P_i(L) \quad \forall t, i = 1...n \tag{10c}$$

In a catalyst pellet, the centre has a plane (ring, slab), line (cylinder) or point (sphere) of symmetry, and the boundary condition Eq. (10b) is of the variable type (von Neumann):

$$z = 0: \frac{\partial P}{\partial z} = 0 \quad \forall t, i = 1...n \tag{10d}$$

Another boundary condition frequently encountered in chemical engineering problems relates the internal transport flux at the gas–particle interface ($z = L$, Eq. (8c)) to the external flux [17,18]. This kind of boundary condition (i.e. the mixed type) is not applied in the present study.

The model given by a set of equations (1), (2) and (9) together with a flux model comprises a set of non-linear, partial differential equations (PDE), which was numerically solved by using a finite-difference technique [19].

3. Comparison of the dusty-gas model, the Fick model, and the Thiele modulus concept for mass transfer accompanied by chemical reaction in porous media with a plane, line or point of symmetry

Irreversible reactions with kinetic rate equations of the type and the transport described according to Eq. (3) is a classical problem and discussed in many standard textbooks [1,2]. Explicit solutions for the interfacial fluxes are available and are generally expressed as the maximum reaction rate in terms of interfacial (bulk) partial pressures multiplied by an effectiveness factor η and a characteristic length δ of the catalyst geometry:

$$N_A = -R(p_{Ai})\delta\eta \tag{11}$$

The effectiveness factor is defined as the ratio of the volume-averaged reaction rate over the maximum reaction rate [1]

$$\eta = \frac{1}{V_{cat} R(p_{Ai})}\int_{V_{cat}} R(p_A)\,\mathrm{d}V \tag{12}$$

For several catalyst geometries, the effectiveness factor can be approximated by a unique function of the Thiele modulus,

$$\eta = \frac{1}{3\phi^2}\left(\frac{3\phi}{\tanh(3\phi)} - 1\right) \quad \text{(sphere)} \tag{13}$$

For nth-order kinetics ($R_A = -k_r p_A^n$) the Thiele modulus is

$$\phi = \delta\left(\frac{(n+1)k_n RT}{2D_A^{e}} p_{Ai}^{n-1}\right)^{1/2}$$

$$\text{with } \delta = r_p/3 \text{ (sphere)} \tag{14}$$

Appropriate expressions were developed for other reaction systems and/or catalyst geometries. Using Eqs. (13) and (14), the flux is easily obtained from Eq. (11). Although this concept is only exact for first-order reactions, it is known as a useful approximation in all other cases. The value of the Thiele modulus reveals information concerning the rate-governing process. If $\phi<0.2$, the transport rate of A is sufficiently high to avoid the occurrence of internal concentration gradients. In this case the reaction has become the rate-governing process and the catalyst area is completely used ($\eta\approx1$). The other limit, $\phi>2$, indicates that the internal transport of components is the rate-governing process and that internal gradients occur. In this region the effectiveness factor is inversely proportional to the Thiele modulus. For the numerical models the concentration profiles are calculated, and the exact value of the effectiveness factor can be directly calculated using Eq. (12), and compared with the approximate solutions.

In the next sections, calculations using the different models for the description of mass transport with chemical reactions in a spherical particle will be presented and discussed for different reaction schemes. The simplest case is the irreversible, binary isomerization reaction $A\rightarrow B$, for which Eq. (13) is exact for first-order kinetics. An extension to the general binary system $A\rightarrow mB$ ($m\neq1$) is made, resulting in a net molar flow through the particle interface. Next, $A+n_BB\rightarrow n_CC+n_DD$ reactions and, finally, multiple reaction schemes and equilibrium reactions are discussed. For catalyst geometries with a symmetrical boundary condition there is no flux of inert species at the interface under steady-state conditions. Hence, it follows directly from the flux expressions that the presence of an inert species does not influence the motion of the other components, and is therefore not taken into account.

3.1. Irreversible reactions of the type $A\rightarrow mB$, with first-order kinetics

The reaction $A\rightarrow mB$ ($m=1$) involves no change in the total number of molecules and so pressure gradients are indeed absent. In this case the DGM can be rewritten as indicated by Eq. (8). Furthermore, the fluxes of A and B are equimolar and in opposite directions. Substitution of this flux ratio in Eq. (8) results in the FM, Eq. (3). As was mentioned above, Eq. (11) with the effectiveness factor calculated according to Eq. (13) now is the exact solution for the flux. Therefore, the effectiveness factor calculated directly from the profiles resulting from the numerical models should equal the result calculated from Eq. (13). This is confirmed by Table 1, which presents the results for slow ($\phi=0.18$), moderate ($\phi=1.3$) and fast ($\phi=4.0$) reactions.

For the general case of $m\neq1$, the reaction involves a net change in the number of molecules, and so a pressure gradient is induced. Substituting Eq. (14) in Eq. (13) to calculate the effectiveness factor is no longer exact, because it neglects the pressure-driven convective motion. Abed and Rinker [20] illustrated that the influence of the pressure gradient on the effectiveness factor depends on the diffusion regime. They showed that, when Knudsen diffusion predominates, the effectiveness factor again depends on the Thiele modulus alone, not on the volume change, and so in this specific regime Eq. (14) remains valid. This was also recognized by Kehoe and Aris [6], who modified the Thiele modulus as

$$\phi'=\phi\left(\frac{m^{1/2}(1+\alpha m^{1/2})}{2\alpha}\right)^{1/2} \tag{15}$$

with

$\alpha=D_{i,k}/D_{ij}$ (ratio of diffusion coefficients)

where $\alpha=D_{i,k}/D_{ij}$ (ratio of diffusion coefficients), which considers the diffusion region via the value of α. Kehoe and Aris [6], and later Hite and Jackson [7], studied the general, irreversible reaction $A\rightarrow mB$ according to the DGM. From approximate analytical solutions they argued that the contribution of a pressure-driven flow to the total transport could be neglected. Therefore, using the generalized modulus, Eq. (15), to calculate the effectiveness factor, Eq. (13), is a reasonable approximation which holds for moderate volume changes. Kehoe and Aris illustrated this for general nth-order kinetics with respect to component A, restricted to a maximum value of $m=4$.

For several reaction rates, the effectiveness factor was calculated according to the present numerical models (extended FM and DGM) and Eq. (13) for model parameters as presented in Table 2. Fig. 1 presents the results for a moderately fast reaction in the transition region. From Fig. 1 it can be concluded that the results of the extended FM are close to the results of the DGM (deviations less than 10%). Variation of the permeability constant B_0 has only a small effect on the fluxes and, consequently, the convective term can be neglected in the transport equation. This is in agreement with Refs. [6,7]. Furthermore, Eq. (12) with the modified modulus, Eq. (15), is a good approximation over a wide range in the case of a net outflow ($m>1$). In the case where is a net inflow ($m<1$), Eqs. (13)

Table 1

	Thiele modulus ϕ		
	4.0042	1.2662	0.1791
η_{exact}	0.22911	0.58264	0.98127
η_{FM}	0.22895	0.58264	0.98127
η_{DGM}	0.22895	0.58264	0.98127

Table 2

$R_0=1.0\times10^{-3}$	$T=600$ K	$P_0=1.0\times10^5$ Pa
$r_p=2.9\times10^{-7}$ m	$\mu=1.0\times10^{-5}$ Pa s	$x_{AR}=1.0$
$B_0=4.79\times10^{-16}$ m^2	$D_{ij}^0=1.5\times10^{-4}$ m^2 s^{-1}	$M_A=20\times10^{-3}$ kg mol^{-1}
$\epsilon/\tau=0.0456$	$D_{i,K}^e=\frac{2\epsilon}{3\tau}r_p\sqrt{\frac{8RT}{\pi M_i}}$ m^2 s^{-1}	$M_B=M_A/m$

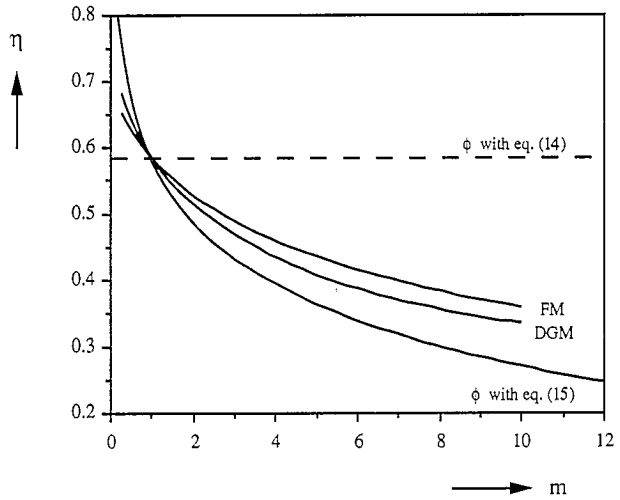

Fig. 1. Effectiveness factor as a function of the number of molecules in the reaction A→mB. The results are shown according to the numerical models, FM and DGM, using Eq. (12), and the approximate solutions, Eq. (13). The results are presented for a moderate reaction rate, spherical particle, and transport in the transition region, $a=1.0$.

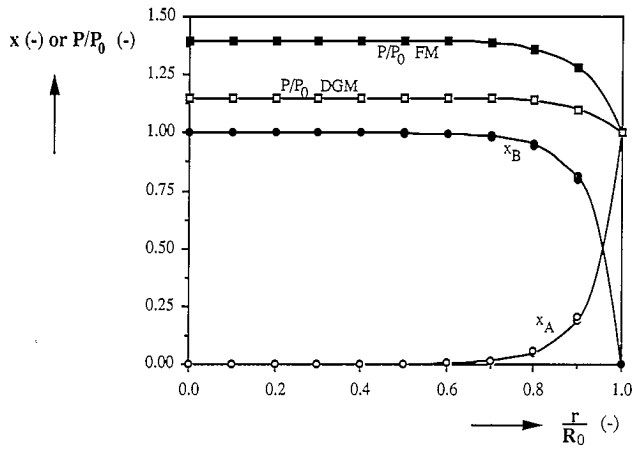

Fig. 2. Dimensionless profiles over the radius of a spherical catalyst particle of components A and B, together with the relative pressure. The results are calculated according to the FM and the DGM for a reaction scheme A→3B and fast kinetics (i.e. $\phi=4.0$, Eq. (14)). The model parameters are presented in Table 2.

and (15) seem to overestimate the increase of the effectiveness factor seriously.

In the Knudsen regime, more extreme intra-particle pressure gradients were calculated, but in this regime the transport depends only on the molecular velocities of the components. Hence, the transport is not affected by these gradients. The maximum pressure in the centre of the pellet was found to be $p_{max}=p_0/m$, which was derived by Hite and Jackson [7]. Also in the case of a poor reaction the discrepancies between the models were small. This is readily explained, since reaction rather than transport determines the interfacial fluxes.

Although the fluxes (and hence effectiveness factor) resulting from the FM and the DGM are approximately the same,. the partial-pressure profiles resulting from these models are generally not. Fig. 2 shows the calculated pressure and mole-fraction profiles over the catalyst particle, resulting from both models, in the case of a fast reaction, A→3B. The mole-fraction profiles practically cannot be distinguished, but the FM calculates a higher total pressure. This can be attributed to a higher contribution of the diffusional transport in the DGM than in the FM, owing to the component interactions. Omitting the pressure gradient term, the explicit result of the DGM for a binary mixture is already presented by Eq. (8). For a reaction A→mB and $m>1$, the term $(1-\gamma x_A)>1$, and therefore the apparent diffusion coefficient of the DGM appears to be greater than the Fick diffusion coefficient according to Eq. (4a). Hence, the diffusive transport in the DGM contributes to a greater extent to the total transport, and the resulting total pressure gradient is lower.

3.2. *Irreversible reactions of the type* $A+n_BB\rightarrow n_CC+n_DD$

Irreversible reactions of multicomponent systems are generally represented by the scheme $A+n_BB\rightarrow n_CC+n_DD$ with arbitrary kinetics. Because the gas mixture is no longer binary, the diffusive transport mechanism clearly differs between the FM and DGM. However, if one component is in excess (diluted systems) only the interaction with this component will be important. In this case the behaviour of the multi-component mixture approximates a binary system, and the results have already been discussed in the previous section. The irreversible reaction $A+n_BB\rightarrow n_CC+n_DD$ was studied for reactions with a substantial difference in molecular mass, e.g. oxidation and (de)hydrogenation reactions of hydrocarbons.

A dehydrogenation reaction A→3H$_2$+B with first-order kinetics, $R_A=-k_rp_A$, was studied as a first example. The model parameters are given in Table 2 and the physicochemical parameters are presented in Table

Table 3

$M_A = 84\times10^{-3}$ kg mol^{-1}	$D^0_{AB} = 1.5\times10^{-4}$ m^2 s^{-1}
$M_B = 78\times10^{-3}$ kg mol^{-1}	$D^0_{iH2} = 7.5\times10^{-4}$ m^2 s^{-1} (i=A,B)
$M_{H2} = 2\times10^{-3}$ kg mol^{-1}	

Table 4

N_{DGM} (mol m^{-2} s^{-1})	N_{FM} (mol m^{-2} s^{-1})	ϕ Eq. (14)	η_{DGM}	η_{FM}	η
0.00328	0.00328	0.142	0.981	0.983	0.955
0.0844	0.0877	0.900	0.632	0.657	0.453
0.629	0.888	6.367	0.124	0.133	0.076

3. Table 4 shows the results for fast, moderate and slow reactions, and the models are in good agreement. The effectiveness factor in the last column of Table 4 was calculated using the modified modulus, Eq. (15), and the A-hydrogen effective, binary diffusion coefficient. As soon as transport limitations occur, the simplified approach, which is based on the Thiele modulus, differs substantially from the numerical calculations. Again the results according to the FM and the DGM are in reasonable agreement for slow, intermediate and fast reactions. For a hydrogenation reaction with overall second-order kinetics, the results of the FM and the DGM agreed within 5% for the corresponding conditions. For this situation the effectiveness-factor concept was not considered because severe linearizations are necessary to obtain expressions for the Thiele modulus [1,2].

Finally, the total oxidation reaction of butane, $6.5O_2 + B \rightarrow 4CO_2 + 5H_2O$ is studied with the model parameters given in Table 2 and the kinetic rate equation according to

$$R_A = \frac{k_r b_A b_B p_A p_B}{(1 + b_A p_A + b_B p_B)^2} \tag{16}$$

in which b_A, b_B are adsorption constants of the reactants (b_A, $b_B > 0$). Bischoff [21] proposed a generalized modulus to be used in Eq. (13) when dealing with more complex kinetics, defined as

$$\phi' = \frac{\delta R_A(p_{A0})}{(2D_A^{eff})^{1/2}} \left[\int_0^{p_{A0}} R(p_A)\, dp_A \right]^{-1/2} \tag{17}$$

Substituting Eq. (16) results in

$$\phi' = \phi \sqrt{\frac{b_B p_{B0}}{2b_A}} \left(\frac{p_{A0}\beta}{p_{A0} + \xi} \right)^2 \tag{18}$$

where $\xi = (1 + b_B p_{B0})/b_A$ and

$$\beta = \left[\ln\left(\frac{\xi + p_{A0}}{\xi} \right) + \frac{\xi}{\xi + p_{A0}} - 1 \right]^{-1/2}$$

Table 5 presents calculations at different values of the reaction rate constant and shows a case with equal adsorption parameters as well as different ones. The effectiveness factor was calculated with respect to oxygen. From these and other calculations, varying the partial pressures of the various components, it could be concluded that the results of the FM are close to the DGM. The effectiveness factor calculated with Eq. (18) is in reasonable agreement with the results of the FM and DGM in both the reaction-controlled regime and the transport-controlled regime. In the transition regime the largest discrepancies are observed, depending also on the magnitudes of the adsorption constants [21]. It also appeared from the numerical models that, although the reaction involves an increase in the number of molecules, the catalyst effectiveness was sometimes observed to be greater than unity. This was caused by a small pressure decrease at low values of reaction rate constant, owing to adsorption of components.

3.3. Multiple reactions in a catalyst particle

The FM always predicted a different pressure profile over the catalyst particle than the DGM (see Fig. 2), whereas the mole-fraction profiles were almost identical. Hence, the local partial pressures resulting from both models are different. Therefore, when the desired reaction is followed by an undesired consecutive reaction the results according to the two models may differ substantially. This was studied for a consecutive reaction scheme, $A + H_2 \rightarrow B + H_2 \rightarrow C$. Hydrogen is involved as a component, so that the components have different mobilities. The kinetic rate equation of the first reaction is overall second-order, first-order with respect to both A and H_2, but the order with respect to the desired product (B) in the consecutive reaction kinetics is taken to be high (third order) in order to make the discrepancies more pronounced. The model parameters

Table 5
Comparison of (oxygen) fluxes and effectiveness factor in case of an oxidation reaction $B + 6.5O_2 \rightarrow 4CO_2 + 5H_2O$, with Langmuir–Hinshelwood kinetics. The Thiele modulus is calculated with respect to oxygen according to the modified equation (18). Model parameters are shown in Table 2 with the addition of: $D_{iB}^0 = 0.3\times10^{-4}$ m^2 s^{-1}; $M_{O2} = 32\times10^{-3}$; $M_{CO2} = 44\times10^{-3}$; $M_{H2O} = 18\times10^{-3}$; $M_B = 58\times10^{-3}$

k_r	ϕ	N_{DGM}	N_{FM}	η_{DGM}	η_{FM}	η
Case I: $b_A = b_B = 10^{-4}$ (Pa^{-1})						
0.5	0.0873	0.0001428	0.0001426	0.997	0.996	0.995
100	1.235	0.01726	0.01731	0.602	0.604	0.592
5000	8.734	0.1557	0.1596	0.109	0.114	0.114
Case II: $b_A = 10^{-3}$; $b_B = 5*10^{-5}$ (Pa^{-1})						
0.5	0.0577	0.0001391	0.0001391	1.003	1.004	0.998
100	0.816	0.02574	0.02730	0.928	0.984	0.743
1000	2.582	0.972	0.1042	0.351	0.376	0.337

together with the results of the calculations are presented in Table 6. In line with the results presented earlier, the fluxes obtained from the two models do not deviate by more than 10% from each other. Hence it can be concluded that, when dealing with multiple reactions, the FM is a good approximation of the DGM as long as only fluxes and/or selectivity are of interest.

A special case of a consecutive reaction occurs when the products recombine again with the reactants, i.e. equilibrium reactions. For equilibrium reactions the transport of the reactants and products inside the porous catalysts, especially the transport differences between the different species, may have a pronounced effect on the composition and hence on the equilibrium conversion. Therefore, also a large number of calculations for this type of reaction have been carried out. From these results, it was observed that, in line with the results of the above-mentioned multiple reactions, the discrepancies between the FM and the DGM remained small (less than 15%).

3.4. Discussion

Modelling mass transport accompanied by chemical reactions in porous catalyst always implies the presence of a pressure gradient. For isobaric diffusion or Knudsen diffusion through a porous medium, Graham's law states

$$\sum_{i-1}^{n} N_i M_i^{1/2} = 0 \tag{19}$$

whereas, when a reaction is involved, the conservation of mass must be obeyed:

$$\sum_{i=1}^{n} N_i M_i = 0 \tag{20}$$

The difference between the two relations is caused by a pressure gradient, albeit small, present in the case where Eq. (20) should hold, i.e. when transport is accompanied by a chemical reaction. Nevertheless, variation of the permeability constant showed that the pressure-gradient term could be neglected in the transport equation (i.e. infinite permeability), in line with the conclusions of Ref. [7]. Only for mechanical reasons is the exact value of the pressure gradient inside the particle of interest.

The concept of the effectiveness factor can only be used as a check whether the entire process of transport accompanied by chemical reaction proceeds in the reaction-controlled regime. When the rate of the total process of transport and chemical reaction inside the catalyst is in either the transition regime or the diffusion-controlled regime, the concept of the effectiveness factor deviates from the numerical calculations according to both the Fick model and the dusty-gas model. In this case, and for multiple reactions as well, it has become necessary to solve the complete set of mass balances for the specific problem. However, a simple Fick model, Eq. (3), with either a constant or a local diffusion coefficient according to Eq. (4b), turned out to be sufficiently accurate to describe the fluxes at the interface and, therefore, the conversion rates.

Table 6
Comparison of the models in case of a consecutive reaction inside the catalyst

Structure parameters	*Reaction mechanism and kinetics*
$r_{cat}= 1.0*10^{-3}$ (m)	$A + H_2 \rightarrow B$ with $R_A= k_r p_A p_{H2}$
$r_{pore}= 5.0*10^{-7}$ (m)	$B + H_2 \rightarrow C$ with $R_B= k_r p_B^3 p_{H2}$
$B_0= 1.54*10^{-15}$ (m^2)	*Conditions at interface*
$\varepsilon/\tau= 4.92*10^{-2}$	$x_A= 0.2$, $x_{H2}= 0.8$, $P= 10^5$ (Pa)

	$k_A(RT)^2= 10$; $k_B(RT)^4= 3$				$k_A(RT)^2= 300$; $k_B(RT)^4= 100$			
model	N_A	N_B	N_{H2}	N_C	N_A	N_B	N_{H2}	N_C
	($mol.m^{-2}.s^{-1}$)				($mol.m^{-2}.s^{-1}$)			
DGM	0.124	0.0755	0.173	0.0489	0.547	0.277	0.817	0.270
FM	0.133	0.0805	0.186	0.0528	0.596	0.303	0.888	0.293

4. Comparison of the dusty-gas model and Fick model for a porous slab facing two different gas-phase compositions

Porous membranes are generally used in separation processes of gaseous components. In contrast to the previous catalyst geometries, the symmetrical boundary condition usually does not occur for porous membranes. For the symmetrical structures the effect of a pressure gradient was concluded to be negligible, but in membrane applications a large pressure gradient over the membrane may give rise to a large convective flow through the membrane. In this case, drift fluxes through the membrane may be present, caused either by a pressure gradient (convective motion) or transport of inert species through the membrane. In symmetrical geometries these effects were absent. Furthermore, owing to the fact that the motion of reactants and products should comply with the stoichiometry, the results of the FM were always close to the DGM. However, the presence of drift fluxes through the membrane can possibly account for larger discrepancies between the models, because this effect is not incorporated in the FM.

Sloot et al. [12] compared the FM with the DGM when dealing with a porous membrane which catalysed an instantaneous equilibrium reaction. They concluded that the deviations between the models became more pronounced at higher mole fractions. For specific process conditions it was observed that a maximum in the deviations occurred, especially when a pressure difference across the membrane was present.

In comparison with Sloot and co-workers [12,18], the present model is more generally applicable because it

is able to incorporate any kinetic rate expression as well as pure diffusion. Similar to Ref. [18], a comparison was made between the FM and the DGM for a porous catalyst having a slab geometry, such as the catalytic membrane reactor configuration. In the calculations at both sides of the membrane a ternary gas was present, and first the transport of the components through the membrane was studied in the absence of a reaction. In this case the effect of the mixture composition on the transport rates was studied. A gas mixture consisting of components with nearly identical physico-chemical properties was discussed as well as with clearly distinct properties. Secondly, a second-order overall irreversible reaction was allowed to proceed between two reactants, separately present at opposite sides of the slab. This situation was studied only for a mixture of components with nearly identical properties. The calculations were restricted to the transition region of diffusion because this is the region of most practical importance for the processes in the membrane reactor. Owing to the fact that transport in the Knudsen regime is similarly incorporated in both models, no differences are observed in this regime.

4.1. Diffusion and convective flow without reaction

Transport of a multicomponent gas through a membrane in the absence of a chemical reaction is studied, with composition as given in Tables 7 and 8. Fluxes through the membrane were calculated according to both the extended FM and the DGM. The boundary conditions were such that there is a net molar flow of the inert through the membrane to make the situation distinct from the transport in the spherical catalyst structure. Two cases were considered, either with a gas mixture consisting of species with nearly identical properties or with hydrogen present, showing a five times higher diffusivity. Depending on the component properties it can be concluded that the differences in the two models are now remarkable.

Table 7

$L_{cat}=2\times10^{-3}$ m
$r_{pore}=2.9\times10^{-7}$ m
$B_0/\mu=1.54\times10^{-10}$ m^2 Pa^{-1} s^{-1}
$\epsilon/\tau=4.92\times10^{-2}$
$T=600$ K
$P=1\times10^5$ Pa

Boundary conditions

	$z=0$	$z=L$
x_A	0.02	0.0
x_B	0.0	0.8
x_{inert}	0.8	0.2

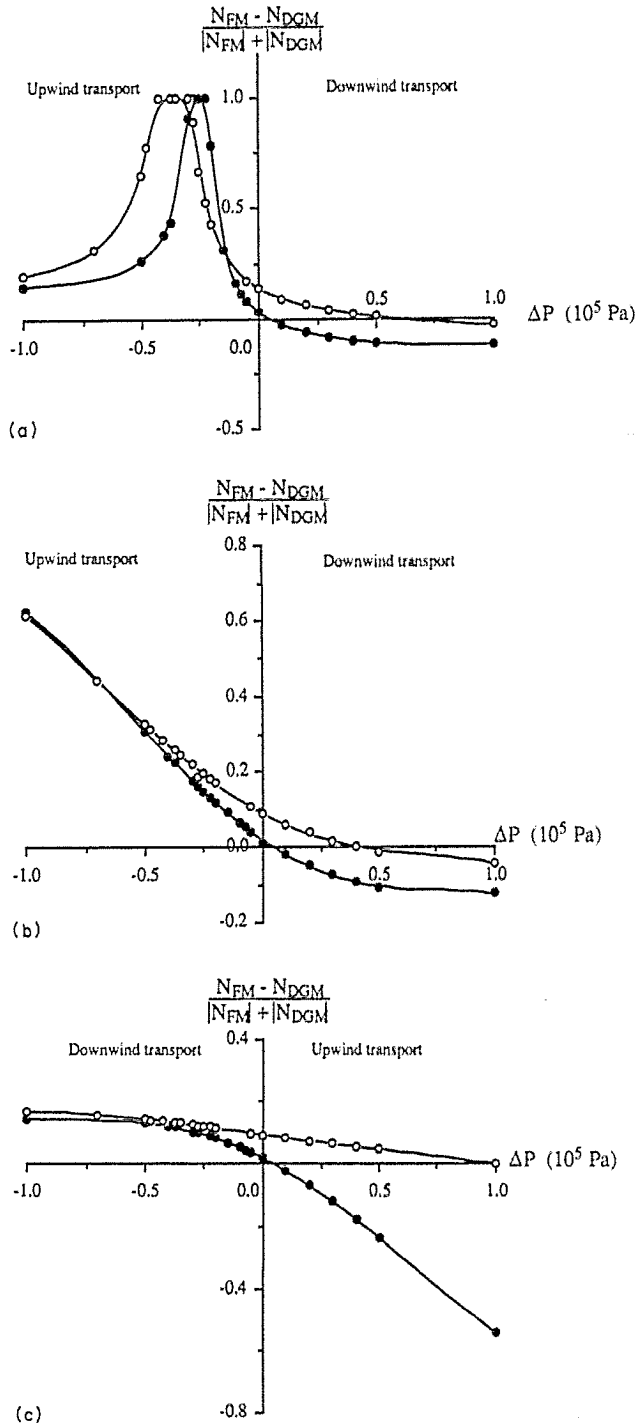

Fig. 3. Relative difference of transport of component A through a membrane in the absence of a reaction, plotted against the transmembrane pressure difference. The results are for a ternary gas mixture with components of identical physicochemical properties (●, inert/A/B) and with hydrogen (○, inert/A/H$_2$): (a) inert transport; (b) transport of A; (c) transport of B.

Fig. 3 shows the differences between the FM and the DGM as a function of the pressure difference for the transport of 'inert' (Fig. 3(a)), A (Fig. 3(b)), and B or hydrogen (Fig. 3(c)). The pressure difference is defined as positive when component A moves down the pressure gradient and its transport is assisted by

Table 8

Identical species	Hydrogen mixture	Reaction parameters
$M_A = M_B = 20 \times 10^{-3}$ kg mol^{-1}	$M_i = 40 \times 10^{-3}$ kg mol^{-1}	$R_A = k_r p_A p_B$ mol m$_{cat}^{-3}$ s^{-1}
$M_C = 40 \times 10^{-3}$ kg mol^{-1}	$M_{H2} = 2 \times 10^{-3}$ kg mol^{-1}	$k_r RT^2 = 1000$
$M_{inert} = 30 \times 10^{-3}$ kg mol^{-1}	$D^0_{iH2} = 7.5 \times 10^{-4}$ m^2 s^{-1}	
$D^0_{ij} = 1.5 \times 10^{-4}$ m^2 s^{-1}	$D^0_{ij} = 1.5 \times 10^{-4}$ m^2 s^{-1}	

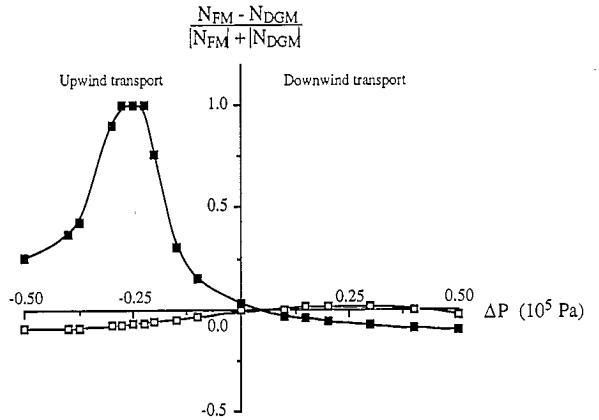

Fig. 4. Relative difference of the models plotted against the pressure difference over the membrane in case a reaction A+B→C proceeds. This figure shows the results for the reactant A (□) and the inert (■) for identical components. Model parameters are shown in Tables 7 and 8.

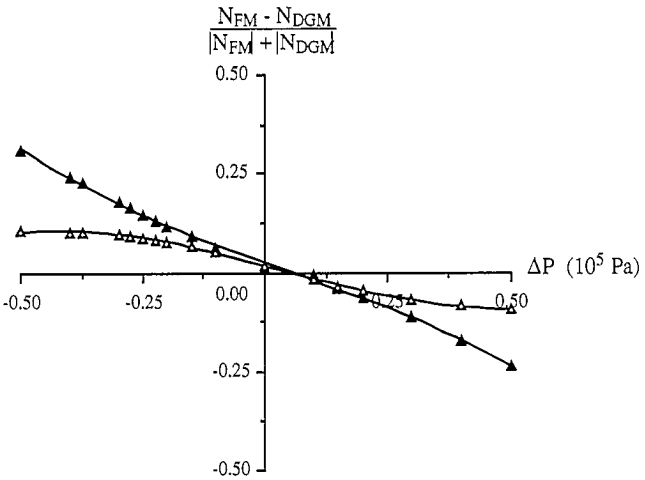

Fig. 5. Relative difference of the product flux directed to the high-pressure side (▲) and to the low-pressure side (△) in a membrane reactor, plotted against the pressure difference. The pressure difference is defined as positive when reactant A moves down the pressure gradient. The reaction scheme reads A+B→C, with model parameters in Tables 7 and 8.

the convective flow. Consequently, components A and 'inert' move upwind at negative pressure differences, and B (or hydrogen) moves upwind at positive values because its partial pressure gradient is opposite to that of both the other components.

From Fig. 3 it can be concluded that the transport of any component moving down the pressure gradient is described by both models equally well. In all cases the deviation curve is close to the Δp axis. As indicated in Figs. 3(b) and 3(c), an increase of the pressure difference across the membrane results in larger deviations. In these diagrams the results of the A, B and hydrogen fluxes are shown. These species cannot be transported against their concentration gradients because they are not present at the opposite side of the membrane. Therefore, these components can only be transported from the membrane interface, by means of a convective flow at sufficiently high pressure differences. The increasing deviation between the models with the pressure difference can be attributed to the Knudsen slip. In the DGM this slip is influenced by the motion of the other components, which is not incorporated in the FM. This effect is more clearly illustrated in Fig. 3(c), where the deviation of the hydrogen flux between the two models is less pronounced. Because hydrogen is a light molecule, its diffusivity has been taken as five times higher than that of the other components. As a result, hydrogen transport is less affected by the transport of other components through the membrane, and hence the deviations between the FM and DGM are less pronounced.

Since the 'inert' is present at both sides of the slab, transport in both directions is possible. As a consequence, Knudsen slip is negligible and the flux predictions at high pressure differences from both models should be in good agreement. This is shown in Fig. 3(a). Large deviations, however, are observed in the case where the pressure gradient balances the concentration gradient and the flux is about to alter its direction. Owing to the fact that the transport is affected by the motion of other species, which is neglected in the FM, the deviations between the models are large.

4.2. Mass transport accompanied by chemical reactions

If the pores of the slab support a catalyst, a reaction can proceed inside the membrane. This resulted in a membrane reactor with separated feed of reactants as described by Refs. [12,13,18,22,23]. The models were studied again for an irreversible reaction A+B→C, with finite reaction rate, proceeding inside the pores, because differences between the models are likely to occur. The boundary conditions were identical to those

used in the previous section and presented in Tables 7 and 8. Also an inert species is present which moves through the membrane, causing a net molar flow. The value of the reaction rate constant is sufficiently high to prevent slip of reactants over the whole range of pressure differences.

The deviation plot of the transport of the inert species and reactant A is shown by Fig. 4. In line with the results presented for the diffusional transport, both models are in good agreement describing the downwind transport. Surprisingly, the upwind transport of component A is also described equally well by both models. This agreement is caused by the reaction because the transport of component A is coupled to the transport of B via the reaction stoichiometry. Reactant A and B cannot move independently of each other through the membrane. This implies a better agreement between the models even in the description of the upwind transport, because one of the reactants is always moving down the pressure gradient. The inert species is not bound to the stoichiometry, and a similar behaviour is observed as in Fig. 3(a).

The product C is able to leave the membrane at either the high-pressure or the low-pressure side. The calculated fluxes to these sides are shown in Fig. 5. In this plot the pressure difference is defined as positive when reactant A moves down the pressure gradient. Consequently, the closed symbols mark the product flux leaving the membrane at the A side at a positive pressure difference, and leaving the membrane at the B side at a negative pressure difference. Fig. 5 again demonstrates that the transport down the pressure gradient is described equally well in both models, whereas the upwind transport is not.

Contrary to transport through porous structures with a plane, line or point of symmetry (catalyst particles), the differences between the FM and the DGM are more pronounced in membranes, caused by drift fluxes. These conclusions are qualitatively in line with those of Ref. [12]. As a result of drift fluxes, the transport of non-reacting species through the membrane as well as the transport direction of reaction products is for some cases severely miscalculated by the FM. From a large number of calculations it can be concluded that the FM overestimates the upwind transport and underestimates the downwind transport. Hence, when modelling gas transport with or without accompanying chemical reactions in two-sided open porous structures, such as (for example) a membrane reactor with separated feed of reactants, the FM cannot be used, although the fluxes of the reactants are in fairly good agreement with the DGM. Only when dealing with very dilute reactant systems do the discrepancies become negligible in all cases, as follows directly from the asymptotic cases of the DGM.

5. Conclusions

From an extensive comparison of the dusty-gas model and the (extended) Fick model for the prediction of interfacial fluxes, or respective effectiveness factors, it could be concluded that pressure effects could be neglected for porous catalyst with a plane, line or point of symmetry. Furthermore, the deviations between the two models were small for these catalyst geometries, so that the simple FM (Eq. (3)) can be used to calculate the fluxes. Expressions for the Thiele modulus were also used to calculate the effectiveness factor, but, although they provide useful approximations, they were accurate only over a limited range.

However, mass transport with and without chemical reactions inside a porous slab facing two different gas phases, resembling catalytic membrane reactors, should be described according to the dusty-gas model. Although the fluxes of the reactants predicted from the Fick model are in reasonable agreement with the dusty-gas model results, the direction of product flows and inert motion through the membrane is not predicted correctly.

Acknowledgements

Financial support for this work was granted by GASTEC, Apeldoorn, The Netherlands, which we gratefully acknowledge. Thanks also to M. Bracht and R.T. Groenland for their contributions in the model calculations and development of the computer program.

Appendix A: Nomenclature

b_A	adsorption constant of component A (Pa^{-1})
B_0	permeability coefficient (m^2)
D_{ij}	binary diffusion coefficient of a mixture i and j ($m^2\ s^{-1}$)
$D_{i,k}$	Knudsen diffusion coefficient of component i ($m^2\ s^{-1}$)
E_{act}	activation energy ($J\ mol^{-1}$)
K_0	Knudsen coefficient (m)
$k_{1,1}$	reaction rate constant of reaction with (1,1)-order kinetics ($mol\ m^{-3}\ Pa^{-2}\ s^{-1}$)
L	membrane thickness (m)
m	stoichiometric coefficient (−)
M_i	molecular mass of component i ($kg\ mol^{-1}$)
n	number of molecules (mol)
N	flux, relative to a fixed coordinate system ($mol\ m^{-2}\ s^{-1}$)
N_v	viscous flow ($mol\ m^{-2}\ s^{-1}$)
P	total pressure (Pa)
p_i	partial pressure of component i (Pa)
R	universal gas constant (=8.314 $J\ mol^{-1}\ K^{-1}$)

R_i reaction rate with respect to component i (mol m^{-3}(cat) s^{-1})
T temperature (K)
t time (s)
x mole fraction (−)
z space coordinate of integration (m)

Greek letters

α ratio of diffusivities D_{ik}/D_{ij} (see Eq. (15))
γ $1+N_B/N_A$ (see Eq. (9))
ϵ porosity (m^3(gas) m^{-3}(cat))
ζ conversion (−)
η effectiveness factor (−)
μ dynamic viscosity (Pa s)
τ tortuosity (−)
ϕ Thiele modulus (−)

Subscripts and superscripts

e effective
i, j, A component
k Knudsen
m mixture
0 gas phase

References

[1] G.F. Froment and K.B. Bischoff, *Chemical Reactor Analysis and Design*, Wiley, New York, 2nd edn., 1990.
[2] K.R. Westerterp, W.P.M. van Swaaij and A.A.C.M. Beenackers, *Chemical Reactor Design and Operation*, Wiley, New York, 2nd edn., 1983.
[3] R.R. Remick and C.J. Geankoplis, *Chem. Eng. Sci., 29* (1974) 1447–1455.
[4] C.F. Feng, V.V. Kostrov and W.E. Stewart, *Ind. Eng. Chem. Fundam., 13(1)* (1974) 5–9.
[5] R. Jackson, *Mass Transport and Reaction in Porous Catalysts*, Elsevier, Amsterdam, 1977.
[6] J.P.G. Kehoe and R. Aris, *Chem. Eng. Sci., 28* (1973) 2094–2098.
[7] R.H. Hite and R. Jackson, *Chem. Eng. Sci., 32* (1977) 703–709.
[8] M.E. Davis, G. Fairweather and J. Yamanis, *Chem. Eng. Sci., 37* (1982) 447–452.
[9] A. Bliek, W.N. Poelje, W.P.M. van Swaaij and F.P.H. van Beckum, *AIChE J., 31* (1985) 1666–1681.
[10] M.G. González, M.A. Laborde and R.J.J. Williams, *Ind. Eng. Chem. Proc. Des. Dev., 19* (1980) 48–501.
[11] G.H. Graaf, H. Scholtens, E.J. Stamhuis and A.A.C.M. Beenackers, *Chem. Eng. Sci., 45* (1990) 773–783.
[12] H.J. Sloot, C.A. Smolders, W.P.M. van Swaaij and G.F. Versteeg, *AIChE J., 38* (1992) 887–900.
[13] H.J. Smolders, C.A. Sloot, W.P.M. van Swaaij and G.F. Versteeg, *J. Membrane Sci., 74* (1992) 263–278.
[14] E.A. Mason and A.P. Malinauskas, *Gas Transport in Porous Media: The Dusty Gas Model, Chemical Engineering Monographs 17*, Elsevier, Amsterdam, 1983.
[15] M. Novák, K. Ehrhardt, K. Klusácek and P. Schneider, *Chem. Eng. Sci., 43* (1988) 185–193.
[16] R.P. Wendt, E.A. Mason and E.H. Bresler, *Bioph. Chem., 4* (1976) 237–247.
[17] R. Cornelisse, A.A.C.M. Beenackers, F.P.H. van Beckum and W.P.M. van Swaaij, *Chem. Eng. Sci., 35* (1980) 1245–1260.
[18] H.J. Sloot, G.F. Versteeg and W.P.M. van Swaaij, *Chem. Eng. Sci., 45* (1990) 2415–2421.
[19] J.W. Veldsink, A catalytically active, non-permselective membrane reactor for kinetically fast, strongly exothermic, heterogeneous reactions, *Thesis*, University of Twente, Enschede, Netherlands, 1993.
[20] R. Abed and R.G. Rinker, *AIChE J., 19* (1973) 618–624.
[21] K.B. Bischoff, *AIChE J., 11(2)* (1965) 351–355.
[22] V.T. Zaspalis, W. van Praag, K. Keizer, J.G. van Ommen, J.R.H. Ross and A.J. Burggraaf, *Appl. Catal., 74* (1991) 249–260.
[23] J.W. Veldsink, R.M.J. van Damme, G.F. Versteeg and W.P.M. van Swaaij, *Chem. Eng. Sci., 47* (1992) 2939–2944.